

Experimental Studies of Ageing in Electrolytic Capacitors

Chetan Kulkarni¹, Gautam Biswas¹, Xenofon Koutsoukos¹, Jose Celaya², and Kai Goebel³

¹ Dept. of EECS, ISIS, Box 351829 Station B, , Vanderbilt University, Nashville, TN 37235, USA
chetan.kulkarni, gautam.biswas, xenofon.koutsoukos @vanderbilt.edu

² SGT, NASA Ames Research Center, MS 269-4, Moffett Field, CA 94035, USA
jose.r.celaya@nasa.gov

³ NASA Ames Research Center, 269-4, Moffett Field, CA 94035, USA
kai.goebel@nasa.gov

ABSTRACT

Understanding the ageing mechanisms of electronic components critical avionics systems such as the GPS and INAV are of critical importance. Electrolytic capacitors and MOSFET's have higher failure rates among the components of DC-DC power converter systems. Our current work focuses on analyzing and modeling electrolytic capacitor degradation and its effects on the output of DC-DC converter systems. The output degradation is typically measured by an increase in ESR (Equivalent Series Resistance) and decrease in the capacitance value over long periods of use even under nominal operating conditions. Typically the primary effect of degradation is increased ripple current and this has adverse effects on downstream components. For example, in avionics systems where the power supply drives a GPS unit, ripple currents can cause glitches in the GPS position and velocity output, and this may cause errors in the Inertial Navigation (INAV) system, causing the aircraft to fly off course. In this paper, we present the details of our ageing methodology along with details of experiments and analysis of the results.

1. INTRODUCTION

Electrolytic capacitors and MOSFET's have higher failure and degradation rates than other components in DC-DC converter systems. The performance of the electrolytic capacitor is strongly affected by its operating conditions, which includes voltage, current, frequency, and working temperature (Lahyani, Venet, Grellet, & Viverge, 1998; Vorperian., 1990). For degraded electrolytic capacitor the impedance path for the ac current in the output filter keeps increasing, thus introducing a ripple voltage on top of the desired output DC voltage (Chen, 2005). Continued degradation of the capacitor leads the converter output voltage to also drop below specifications and in some cases the combined effects of

the voltage drop and the ripples may damage the converter itself in addition to affecting downstream components. The paper develops a method for studying the degradation effects of electrolytic capacitors subject to loading under nominal operating conditions and their impact on overall system performance.

The output degradation in the DC-DC converters is typically measured by the increase in ripple current and the drop in output voltage at the load. Typically the ripple current effects dominate, and they can have adverse effects on downstream components. The work in this paper is specifically directed towards DC-DC converters in Avionics systems. In these systems the power supply drives a Global Positioning System (GPS) and INAV unit, and ripple currents at the converter output can cause glitches in the GPS position and velocity output, and this, in turn, may cause errors in the Inertial Navigation (INAV) system causing the aircraft to fly off course (Kulkarni, Biswas, Bharadwaj, & Kim, 2010).

Switched-mode power supplies are widely used in DC-DC converters because of their high efficiency and compact size. DC-DC converters are important in portable electronic devices, which derive their power primarily from batteries. Such electronic devices often contain several sub-circuits with different voltage requirements (sometimes higher and sometimes lower than the supply voltage, and possibly even negative voltage). DC-DC converters can provide additional functionality for boosting the battery voltage as the battery charge declines. A typical buck-boost DC-DC converter schematic circuit is illustrated in Fig. 1.

In general, capacitor degradation has been studied under nominal conditions as well as under stress, such as high voltage, high ripple, and adverse thermal conditions (Kulkarni, Biswas, & Koutsoukos, 2009; Hayatee, 1975). Our overall goal is to perform a systematic study of capacitor degradation under nominal and stress conditions by replicating and extending some of the experimental studies that have been carried out in the past. Our approach is to perform empirical studies and then link them to theoretically-derived physics of failure models. This paper presents a first step by systematically collecting capacitor degradation data under nominal operating conditions. The results are mapped to an em-

This is an open-access article distributed under the terms of the Creative Commons Attribution 3.0 United States License, which permits unrestricted use, distribution, and reproduction in any medium, provided the original author and source are credited.

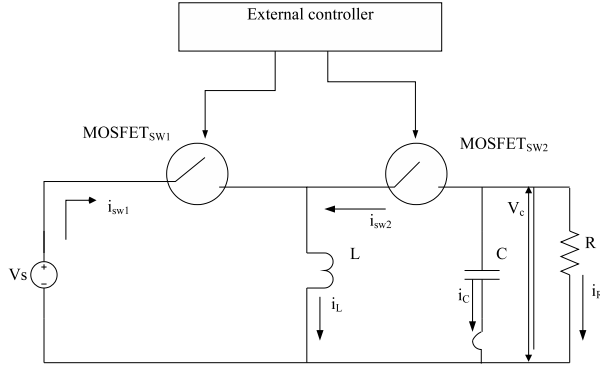


Figure 1: Buck Boost Converter Schematic Circuit

pirical physics of failure model based on Arrhenius law for ESR degradation (Venet, Darnand, & Grellet, 1993). We present preliminary empirical results for capacitance degradation in this paper as a first step to studying capacitance degradation using physics of failure models. The experimental studies, conducted at the NASA Ames Prognostics Centre of Excellence Lab, are discussed in greater detail later in the paper.

The rest of this paper is organized as follows. The following section discusses the mechanisms for capacitor degradation in DC-DC converters. The next section discusses the degradation experiments conducted on electrolytic capacitors. The following sections discuss the analysis methods on the empirical data from the experiments. The paper concludes with discussion of the results and future work.

2. ELECTROLYTIC CAPACITOR DEGRADATION

This section discusses in detail the conditions under which the capacitor degrades leading to faults in the system. We study the adverse effects of the load conditions, operating conditions, ripple currents, which cause degradation by raising the temperatures in the capacitor core.

2.1 Physical Model of the Capacitor

An aluminum electrolytic capacitor, illustrated in Fig. 2 consists of a cathode aluminum foil, electrolytic paper, electrolyte, and an aluminum oxide layer on the anode foil surface, which acts as the dielectric. When in contact with the electrolyte, the oxide layer possesses an excellent forward direction insulation property (Gasperi, 1996). Together with magnified effective surface area attained by etching the foil, a high capacitance is obtained in a small volume (Fife, 2006).

Since the oxide layer has rectifying properties, a capacitor has polarity. If both the anode and cathode foils have an oxide layer, the capacitors would be bipolar (Chen, 2004). In this paper, we analyze the ‘non-solid’ aluminum electrolytic capacitors in which the electrolytic paper is impregnated with liquid electrolyte. There is another type of aluminum electrolytic capacitor, that uses solid electrolyte but we will not include these types of capacitors in this discussion (Bengt, 1995).

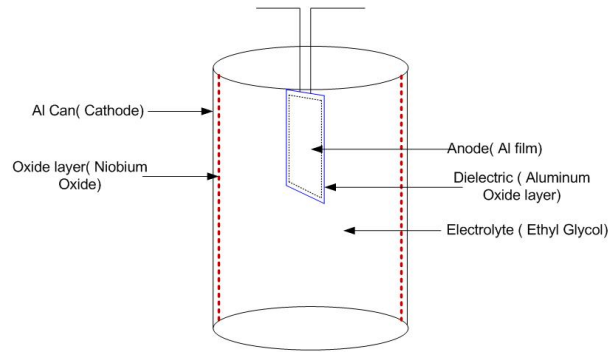


Figure 2: Physical Model of Electrolytic Capacitor.

2.2 Degradation Mechanisms

There are several factors that cause degradation in electrolytic capacitors. As the degradation increases time the component fails, and this impacts the overall system functionality. Failures in a capacitor can be one of two types: (1) catastrophic failures, where there is complete loss of functionality due to a short or open circuit, and (2) degradation failures, where there is gradual deterioration of capacitor function. Degradations are linked to an increase in the equivalent series resistance (ESR) and decrease in capacitance over time (Brettle & Jackson, 1977; Luo, Namburu, Pattipati, & et'al, 2003). Some of the causes of degradation and their related symptoms are discussed below:

1. High Voltage conditions: The capacitance decreases and ESR increases.
2. Transients: The leakage current can be high and an internal short-circuits can occur.
3. Reverse Bias: The leakage current becomes high with loss of capacitance and increase in ESR.
4. Strong Vibrations: These can cause internal short circuits, capacitance losses, high leakage currents, increase in ESR and open circuits.
5. High Ripple current: These cause internal heating, increasing the core temperature which results in gradual aging of the capacitor.

A primary reason for wear out in aluminum electrolytic capacitors is due to vaporization of electrolyte, which, in turn leads to a drift in the main electrical parameters of the capacitor. One of the primary parameters is the equivalent series resistance (ESR). The ESR of the capacitor is the sum of the resistance due to aluminum oxide, electrolyte, spacer, and electrodes (foil, tabbing, leads, and ohmic contacts)(Hayatee, 1975; Gasperi, 1996). The health of the capacitor is often measured by the ESR value. Over the operating period, the capacitor degrades, i.e., its capacitance decreases and ESR increases. Considering the current ESR value and operating conditions the remaining useful life of the capacitor can be calculated using model-based methods.

There are certain industry standards for these parameter values, if the measurements exceed these standards then the component is considered failed, i.e., the component has reached its end of life, and should be immediately replaced before further operations (Lahyani et al., 1998; Eliasson, 2007; Imam, Habetler, Harley, & Divan, 2005). The next section discusses in detail the experiments being conducted on the DC-DC converter hardware to study and measure the degradation of the relevant capacitor parameters.

3. CAPACITOR DEGRADATION EXPERIMENTS

To observe the degradation phenomenon we carried out experiments with the actual DC-DC converter hardware (Kulkarni, Biswas, Koutsoukos, Goebel, & Celaya, 2010). This experiment was conducted to determine capacitor degradation in DC-DC converters when working at room temperature and prolonged operating time. The DC-DC converter used for the experiments was purchased off the shelf, which met the specifications for the experiment. Figure 3 shows the schematic diagram of the hardware setup used for the nominal degradation experiment.

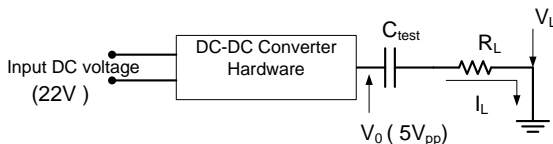


Figure 3: DC-DC converter Hardware : Schematic

Under nominal conditions, the DC-DC converter has a variable input from 22V-36V DC and gives an output of 5V with 1% ripple and noise. Figure 4 shows the DC-DC converter hardware used for the experiment. The configuration for the experimental hardware is similar to the schematic of the DC-DC converter presented earlier in paper. The main hardware components include the MOSFET's, isolating transformers, pulse width modulation (PWM) controller chip and the filter electrolytic capacitor at the output. The filter capacitor is the component under study for degradations. The capacitor is subjected to stresses that occur due to extended operations at room temperature.

3.1 Measurements

The ESR measurements were made approximately every 20-30 hours of operation time. As the experiment time reached 3000 plus hours we started taking more frequent readings to capture the degradation phenomenon of the capacitors. Early on we took one measurement set per day and from the period beyond 3000 hours we increased this frequency to two reading per day. The ambient temperature for the experiment was controlled and kept at 25°C throughout the experiments period.

For taking the measurements each time the whole setup is shutdown and the capacitors are discharged completely before any measurements. The capacitors are then taken out from the boards for the measurements to be taken using the EIS measurement instrument. After

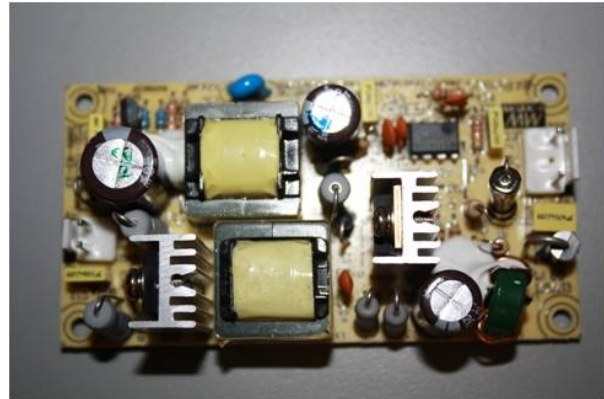


Figure 4: DC-DC converter Hardware

taking the measurements all the capacitors are again replaced to their respective positions and the experiment is restarted under the same conditions. Removing the capacitors from rest of the circuits and taking measurements avoids any other impedances being added to the measurement and recording more accurate readings. The measured ESR values were computed by averaging the real part of the measurements, the capacitor value was computed from the imaginary part of the measured signals using Electrochemical Impedance Spectroscopy Z-Fit mentioned earlier.

This was done for all the three capacitors under test. Keeping all the conditions intact the experiment was started again till the next measurement. This procedure was followed and recorded for all the readings taken during the time of the experiment.

3.2 Experiment: Nominal Degradation

Three sets of DC-DC converter hardware units were considered for the experiment as discussed earlier. Electrolytic capacitors of 2200 μ F capacitance, with a maximum rated voltage of 10V, maximum current rating of 1A and maximum operating temperature of 85°C was used for the study. This was the suggested type of capacitor by the manufacturer of the hardware. The capacitors used for the experiments were picked from the same lot of one manufacturer, and all the capacitors in the lot had similar specifications. The pristine capacitors under test were measured for initial ESR and capacitance value with other related measurement details before the start of the experiment at room temperature using the EIS instrument. As per the specifications in the data sheets both the ESR and capacitance measurements are to be done at 100KHz. In our experimental setup we made a sweep of frequency from 10KHz - 100KHz for all the measurements and values are reported for the highest frequency. Fig. 5 shows the actual test setup for the three units of DC-DC converters under test.

The ESR and capacitance measurements were taken using a SP-150 Biologic SAS measuring instrument. The average initial ESR value was measured to be around 49m Ω and average capacitance of 2068 μ F for the three electrolytic capacitors under test. The electrolytic capacitor is considered as a series RC circuit. The ESR value is real impedance measured through the terminal software of the instrument. Similarly the capacitance

value is computed from the imaginary impedance using Electrochemical Impedance Spectroscopy(EIS) Z-Fit.

These values are calculated directly at the time of measurement or later off-line. In this experiment we recorded the capacitor degradation under normal operating conditions over the period of time which was clocked to about 3000 plus hours of operation time.

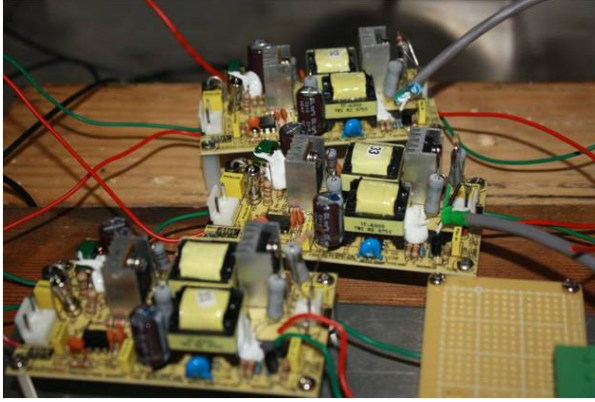


Figure 5: Experimental Setup for 3 DC-DC converter Units

The input DC voltage is supplied from a steady voltage source. A constant input voltage of 22V was supplied to the converter. At the output, the measured voltage was a constant value of 5V with the ripples within the accepted noise tolerance of 1%. We build three DC-DC converters and put them under test at the same time, and the measurements for all the three capacitors on these converters were taken at the same time intervals.

4. DATA ANALYSIS

All the data collected was analyzed to observe how the ESR and the capacitance were changing over the period of time. As per the industry standards, capacitors are considered completely degraded and not usable in the circuit when it's ESR value reaches 2.8 times of the initial ESR value measured. In case of capacitance threshold, the value should not go below 20% of the initial value after which the capacitor is considered to be unhealthy to be used in the circuit. Our goal is to continue the experiment to capacitor failure, but we have not reached that point yet.

From the collected data over the period of time we can then extrapolate the remaining useful life of the capacitor under normal operating conditions. Thus with this data we predict approximately the capacitor degradation rates, and the time to failure.

4.1 ESR Data Analysis

Table 1 shows the average percentage increase and average increase in ESR value over the period of operation.

Since the three capacitors and the converter units were subjected to similar conditions of temperature, input voltage and load, we averaged the collected data and the table discusses the same. (*Please note the ESR values have been rounded till the third decimal just for the tables, but actual values have been used during the calculations and plotting of the data.*)

Table 1: Average Percentage ESR increase and Average ESR value

Time (Hours)	ESR(m Ω)	% ESR Increase
0	0.049	0
200	0.051	3.371
400	0.053	7.66
600	0.056	11.10
800	0.057	15.27
1000	0.059	18.76
1200	0.060	21.97
1400	0.062	25.73
1600	0.064	29.63
1800	0.066	33.26
2000	0.068	37.33
2200	0.070	42.24
2400	0.073	46.95
2600	0.076	53.60
2800	0.079	60.57
3000	0.083	66.68
3200	0.087	72.22
3400	0.093	78.97
3600	0.102	102.95

Figure 6 shows the plot for the percentage increase in the ESR value for each of the three capacitors and their mean percentage increase for the given operation period.

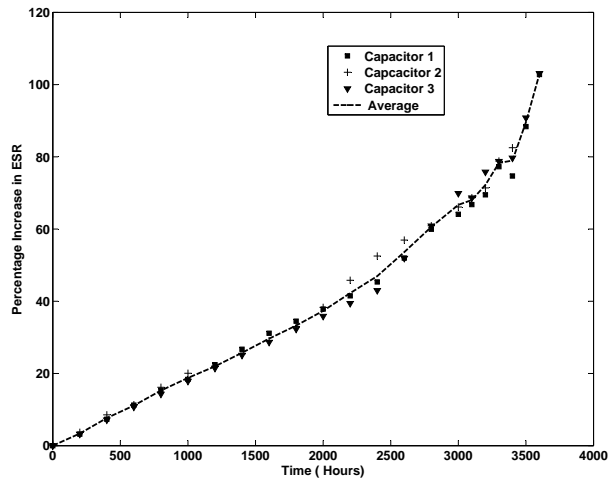


Figure 6: Percentage variation in ESR value for 3 capacitors under test

The data as discussed earlier was collected at 20-30 hour intervals. Initially the increase in ESR value and the decrease in capacitance values were small, but as time progressed the degradation rate increased. The data shown Table 1 are the measured ESR values at 200 hour intervals.

Fig. 7 shows the plot for the average increase in the ESR values for all the three capacitor units for the experimental period. It is observed that till 3200 hours of operation we observed almost a linear increase in the ESR value of the capacitor. Thus the predicted degradation till

this operating time produced an almost linear equation curve fit. After 3200 hours there was a greater increase in the ESR values. The plots illustrate these changes for all three capacitors.

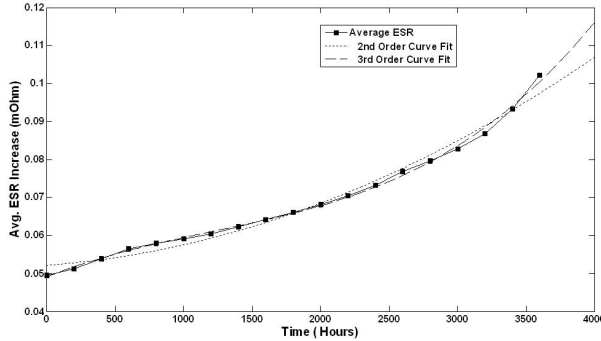


Figure 7: Degradation in ESR parameter

At the end of 3600 hours of operation the average capacitor ESR value increased by approximately 102% of the initial value. At present this experiment is still in progress and we are monitoring the parameters to observe further degradation phenomenon more clearly.

The data analyzed from the experiments was compared with the Arrhenius Law (Venet et al., 1993). Our previous work (Kulkarni, Biswas, Koutsoukos, et al., 2010) dealt with the experimentation involving Arrhenius Law. A linear inverse model derived as an extension of Arrhenius Law to define the change in ESR value over the period of time for a capacitor subjected to a constant operating temperature was used (Jones & Hayes, 1987; Rhoades & Smith, 1984; Gasperi, 1996). The linear inverse model for computing ESR value at time 't' for a given temperature T is given by:

$$\frac{1}{ESR_t} = \frac{1}{ESR_0} \left(1 - k.t.exp\left(\frac{-E}{T+273}\right) \right) \quad (1)$$

where :

- ESR_t = the ESR value at time 't'.
- T = the temperature in °C at which the capacitor operates.
- t = the operating time.
- ESR_0 = initial ESR value at t = 0.
- k = constant which depends on the design and the construction of the capacitor.
- E = is the activation energy/ Boltzmann's constant and equals 4700 (Rhoades & Smith, 1984).

The factor k depends the design and size of the capacitor used. The value of k is typically determined empirically for a particular class of capacitors (Kulkarni, Biswas, Koutsoukos, et al., 2010).

Table 2 shows the average ESR value measured from the experiments compared with the values calculated using the Arrhenius Law equation. It is observed that the calculated values are comparable to the experimental value data. In the next section we discuss the decrease in capacitance value.

Table 2: Experimental and Calculated ESR (mΩ) values

Time (Hours)	Experimental	Calculated
0	0.049	0.0495
200	0.051	0.0509
400	0.053	0.0524
600	0.056	0.0541
800	0.057	0.0558
1000	0.059	0.0576
1200	0.060	0.0596
1400	0.062	0.0618
1600	0.064	0.0639
1800	0.066	0.0664
2000	0.068	0.0689
2200	0.070	0.0718
2400	0.073	0.0749
2600	0.076	0.0782
2800	0.079	0.0819
3000	0.083	0.0858
3200	0.087	0.0903
3400	0.093	0.0952
3600	0.102	0.1007

4.2 Capacitance Data Analysis

In the last section we studied analysis for the ESR parameter. Similarly in this section we will analyze the capacitance parameter in detail. Figure 8 shows the percentage decrease in each of the three capacitors under test. The dashed line shows the average capacitance decrease during the given period of operation time.

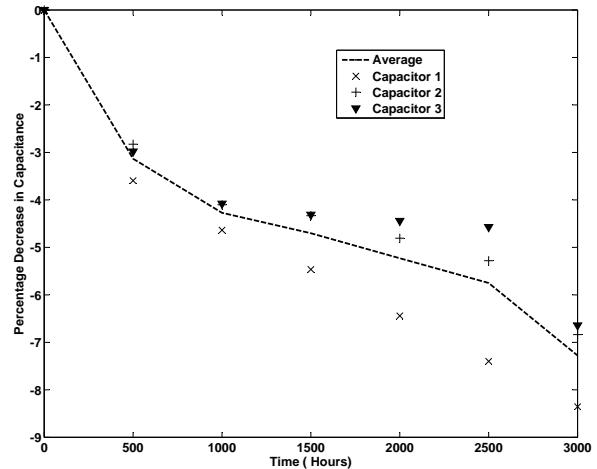


Figure 8: Percentage variation in Capacitance values for 3 capacitors under test

Table 3 shows the average percentage decrease in the values of the capacitance over the period of operation. The table shows the decrease in the capacitance over 500 hour interval for a total of 3000 hours operation. (Please note the capacitance values have been rounded till the third decimal just for the tables, but actual values have been used during the calculations and plotting of the data.)

At the end of 3000 hours it was observed that the aver-

Table 3: Average Percentage decrease and Average Capacitance value

Time (Hours)	% Decrease	Value (μF)
0	0	2068
500	3.133	2000
1000	4.272	1978
1500	4.702	1967
2000	5.229	1955
2500	5.750	1944
3000	7.278	1913

age capacitance decreased by approximately 7.3%. Implementing the curve fitting for data we can then use the equations for approximate degradation failure.

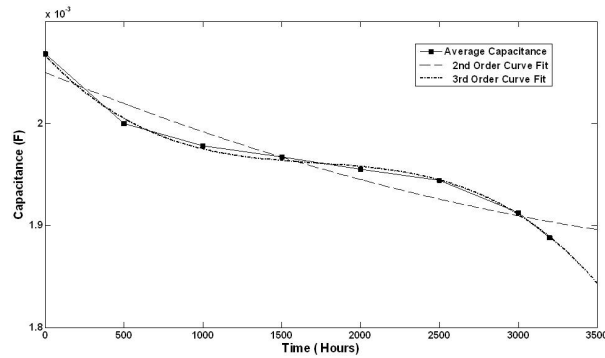


Figure 9: Degradation in Capacitance value parameter

Figure 9 shows the plot for the average capacitance of the three capacitor units. With reference to the average capacitance data a quadratic fit (second order) and cubic fit (third order) was done for the data. From the least squares calculation it was found that the cubic fit matched the experimental data in the best manner. The equation for the degradation data approximation is given as below.

$$\begin{aligned}
 y = & -2.8 * 10^{-5} * \left[\frac{(t - 1.7 * 10^3)}{1.2 * 10^3} \right]^3 \\
 & - 2.1 * 10^{-8} * \left[\frac{(t - 1.7 * 10^3)}{1.2 * 10^3} \right]^2 \\
 & - 1.2 * 10^{-5} * \left[\frac{(t - 1.7 * 10^3)}{1.2 * 10^3} \right] + 0.002
 \end{aligned} \quad (2)$$

where :

y = Capacitance value at time 't'.

t = Time in Hours.

From the plot for capacitance decrease and the third order equation we observe that in earlier stages of experiment, first and third order combined are dominant which we see in the linear decrease of the capacitance value. As the time period increases the third order dominates the capacitance values and it starts decreasing rapidly as observed at the knee point right after 2500 hours of operation. This rapid decrease could be related to the decrease in the volume of the electrolyte. At present this is the

preliminary work related to capacitance decrease as observed from the measurement. Our future work will be focused to relate this rapid decrease to change in volume of the electrolyte.

5. CONCLUSION AND FUTURE WORK

In the paper we discuss how it is important to observe the degradation phenomenon in electronic components specifically used in avionics systems. Our goal in this work was focussed on studying the degradation of electrolytic capacitors under nominal conditions and implement this data to study and predict end of life for the capacitors under test. From the experimental measurements we compared the recorded ESR data with the Arrhenius equation and the data was seen to be comparable with the equation. Similarly there was no specific model to compare for the decrease in the capacitance. The data recorded was then compared with the second and third order curve fits to obtain the degradation equation. As discussed from the data plots observed above by fitting the curves we can approximately predict the time when the capacitor will reach its end of life.

This recorded decrease in the capacitance and increase in the ESR affects the output ripple voltage of the converter. As these components change the RC time constant changes leading to increase in the output ripple voltage thus affecting components down the line. While still the experiments are in progress we intend to collect more data and make more efficient predictions using the existing collected data from experiments.

Our further study goal is to look at accelerated degradations due to stressors like high voltage and high temperature conditions. We are working on setting up experiments and do a similar study as done in the present work. After conducting the experiments and analyzing the data we can then predict the end of life under these varying operating conditions and combine the models together. These can then be used in our MATLAB/SIMULINK[®] models to study the cascading effect of this degradation on the avionics subsystems like GPS and INAV.

ACKNOWLEDGMENTS

The experiments for this paper were conducted at the Prognostics Center of Excellence, NASA Ames Research Centre. This project was funded by NASA NRA # NNX07ADIZA, where Vanderbilt has a subcontract from Honeywell Labs, Minneapolis. We thank Raj Bharadwaj, PI for the project for his helpful suggestions. We are also thankful to Trevor Hutchins for his time and efforts at the Ames Prognostic Lab in taking the readings for the experiments during the period.

REFERENCES

- Bengt, A. (1995). Electrolytic Capacitors Theory and Applications [Computer software manual]. Sweden.
- Brettell, J., & Jackson, N. F. (1977). Failure Mechanisms in Solid Electrolytic Capacitors. *Electrocomponent Science and Technology*, 3, 233- 246.
- Chen. (2004). Ripple Current Confusion [Computer software manual].

- Chen. (2005, Oct). Electrolytic Capacitor Failure Prediction of LC filter for Switching-Mode Power Converters. *Industry Applications Conference, 2005. Fortieth IAS Annual Meeting*, 2(2), 1464 - 1469.
- Eliasson, L. (2007, October - November). Aluminium Electrolytic Capacitor's performance in Very High Ripple Current and Temperature Applications. *CARTS Europe 2007 Symposium, Spain*.
- Fife, J. (2006, Aug). *Wet Electrolytic Capacitors* (Patent No: 7,099 No. 1). Myrtle Beach, SC: AVX Corporation.
- Gasperi, M. L. (1996, October). Life Prediction Model for Aluminum Electrolytic Capacitors. *31st Annual Meeting of the IEEE-IAS*, 4(1), 1347-1351.
- Hayatee, F. G. (1975). Heat Dissipation and Ripple Current rating in Electrolytic Capacitors. *Electrocomponent Science and Technology*, 2, 109-114.
- Imam, A., Habetler, T., Harley, R., & Divan, D. (2005, June). Condition Monitoring of Electrolytic Capacitor in Power Electronic Circuits using Adaptive Filter Modeling. *IEEE 36th Power Electronics Specialists Conference, 2005. PESC '05.*, 601-607.
- Jones, J. A., & Hayes, J. A. (1987). The parametric drift behavior of aluminum electrolytic capacitors: An evaluation of four models. *1st European Capacitor and Resistor Technology Proc, Brighton, U.K.*, 171-179.
- Kulkarni, C., Biswas, G., Bharadwaj, R., & Kim, K. (2010, April). Effects of Degradation in DC-DC Converters on Avionics Systems: A Model Based Approach. *Machinery Failure Prevention Technology Conference, MFPT 2010*, 8-13.
- Kulkarni, C., Biswas, G., & Koutsoukos, X. (2009, October). A prognosis case study for electrolytic capacitor degradation in DC-DC converters. *PHM Conference 2009*.
- Kulkarni, C., Biswas, G., Koutsoukos, X., Goebel, K., & Celaya, J. (2010, February). Physics of Failure Models for Capacitor Degradation in DC-DC Converters. *The Maintenance and Reliability Conference, MARCON 2010*.
- Lahyani, A., Venet, P., Grellet, G., & Viverge, P. (1998, Nov). Failure prediction of electrolytic capacitors during operation of a switchmode power supply. *IEEE Transactions on Power Electronics*, 13, 1199-1207.
- Luo, J., Namburu, M., Pattipati, K., & et'al. (2003, Sep). Model-based Prognostic Techniques. *AUTOTEST-CON 2003. IEEE Systems Readiness Technology Conference. Proceedings*, 330- 340.
- Rhoades, G. E., & Smith, A. W. H. (1984). Expected life of capacitors with nonsolid electrolyte. *34th Component Conf. Proc*, 156-161.
- Venet, P., Darnand, H., & Grellet, G. (1993). Detection of faults of filter capacitors in a converter. Application to predictive maintenance. *INTELEC Proc*, 2, 229-234.
- Vorperian., V. (1990, May). Simplified analysis of pwm converters using model of pwm switch.continuous conduction mode. *IEEE Transactions on Aerospace and Electronic Systems*, 490496.